

1 Manuscript was completed on the 21<sup>st</sup> of April 2020.

2 **Discussion on the separation of macropores and micropores in a compacted expansive clay**

3 Shengyang Yuan<sup>1</sup>, Xianfeng Liu<sup>2</sup>, Enrique Romero<sup>3</sup>, Pierre Delage<sup>4</sup>, Olivier Buzzi<sup>5</sup>

4 **Affiliations:**

5 <sup>1,2</sup>Key Laboratory of High-speed Railway Engineering of Ministry of Education, School of  
6 Civil Engineering, Southwest Jiaotong University, Chengdu 610031, China.

7 <sup>1,2,5</sup>Priority Research Centre for Geotechnical Science and Engineering, The University of  
8 Newcastle, University of drive, Callaghan, NSW, 2308, Australia.

9 <sup>3</sup>Department of Geotechnical Engineering and Geosciences, Universitat Politècnica de  
10 Catalunya, Barcelona Spain.

11 <sup>4</sup>Ecole des Ponts ParisTech, 6–8 av. Blaise Pascal, Cité Descartes, Champs-sur-Marne, F-  
12 77455 MARNE LA VALLEE, France.

13 <sup>1</sup>Associate Professor, Email: [shengyang.yuan@swjtu.edu.cn](mailto:shengyang.yuan@swjtu.edu.cn)

14 <sup>2</sup>Professor, Email: [Xianfeng.liu@swjtu.edu.cn](mailto:Xianfeng.liu@swjtu.edu.cn)

15 <sup>3</sup>Professor, Email: [enrique.romero-morales@upc.edu](mailto:enrique.romero-morales@upc.edu)

16 <sup>4</sup>Professor, Email: [pierre.delage@enpc.fr](mailto:pierre.delage@enpc.fr)

17 <sup>5</sup>Professor, Email: [olivier.buzzi@newcastle.edu.au](mailto:olivier.buzzi@newcastle.edu.au)

18

19 **Corresponding author: Dr. Xianfeng Liu, [Xianfeng.liu@swjtu.edu.cn](mailto:Xianfeng.liu@swjtu.edu.cn)**

20 Main text contains 2119 words

21 6 Figures, 3 Tables.

22

23 **Abstract:**

24 The behaviour of clayey soils is strongly correlated to their microstructure and evolution  
25 thereof. Microstructural investigations have contributed to understanding soil behaviour and  
26 have supported the development of multi-scale coupled models. One of the most accessible  
27 methods to characterize soil microstructure is mercury intrusion porosimetry, which provides  
28 a pore size distribution (PSD) ranging from few nanometers to several hundreds of micrometers.  
29 PSDs can be used to compute micro and macro strains or simply to estimate, in aggregate  
30 microstructures, the void ratios associated to macro pores and micro pores. However, in both  
31 cases, a boundary has to be set to separate the different pore populations. This paper discusses  
32 some criteria that have been proposed in the literature to separate the pore populations. The  
33 discussion is illustrated with extensive micro structural data obtained for Maryland clay. The  
34 paper highlights the effect of initial conditions and boundary conditions on the delimiting  
35 diameter given by some of the criteria. It is also shown that using different criteria will yield  
36 different values of delimiting pore size, with a risk of obtaining unrealistic estimates of micro  
37 and macro void ratios and strains. Finally, it is suggested to account for known soil behaviour  
38 to interpret microstructural data.

39 **List of notations:** not applicable.

40 **Key words:** expansive soils, swelling, microstructure, MIP, SEM, micropores, macropores

41

42 **1- Introduction**

43 A remarkable number of studies have investigated the microstructure of clayey soils and its  
44 evolution under wetting, drying, aging or changes in effective stress (Diamond, 1970;  
45 Sridharan et al., 1971; Ahmed et al., 1974; Delage and Lefebvre 1984; Griffith and Joshi 1989,  
46 Simms and Yanful, 2001; Agus and Schanz, 2005; Delage et al., 2006; Koliiji et al., 2006; Thom  
47 et al., 2007; Li and Zhang, 2009; Romero, 2013). Mercury intrusion porosimetry (MIP) is  
48 commonly used for microstructural analysis of dehydrated soils (often by freeze-drying,  
49 Zimmie and Almaleh, 1976; Delage and Pellerin, 1984; Yuan et al., 2018) because of the large  
50 range of pore size covered (3.5 nm to 0.4 mm). Raw MIP data consists of the evolution of  
51 cumulative volume of intruded mercury per gram of specimen with mercury injection pressure,  
52 which is turned into an entrance pore diameter using Laplace-Young's equation. Multiplying  
53 the cumulative volume of intruded mercury per gram of soil by the unit mass of soil solid

54 particles result in the intruded void ratio, here note  $e_{MIP}$ . The first derivative of intruded void  
55 ratio with respect to logarithm of entrance pore diameter corresponds to the pore size density  
56 function of sample. Its relative ease of use and the fact that it provides an overall pore size  
57 distribution of the specimen, rather than some local surficial information (Romero and Simms,  
58 2009).

59 In parallel to experimental studies, a number of models have been developed (e.g. Alonso et  
60 al., 1999; Yong, 1999; Simms and Yanful, 2002; 2005; Sanchez et al., 2005; Romero et al.,  
61 2011; Casini et al., 2012; 2013; Della Vecchia et al., 2013; Masin, 2016) to account for  
62 couplings between macropores and micropores. However, distinguish micropores and  
63 macroopres is not always straightforward and different criteria have been adopted by various  
64 authors.

65 The literature contains little information on the variability of answers given by the different  
66 criteria, the effect of selecting one criterion over another and the parameters that can affect the  
67 selection of a criterion.

68 In this paper, five different criteria are applied to microstructural data recently obtained on  
69 Maryland Clay (Burton et al., 2015; Yuan et al., 2016; 2019a; 2020) in order to discuss the  
70 variability of delimiting diameter obtained and the effect of initial and boundary conditions on  
71 some criteria. Observations are made to guide researchers to decide on how to select an  
72 appropriate delimiting diameter. Very importantly, the separation between pores should not be  
73 considered solely in terms of pore size but, rather, from behavioural features, related to water  
74 adsorption or volume change, for example.

75

76

## 77 2- Material and experimental data

78 The different criteria are discussed using MIP data obtained on compacted Maryland clay  
79 (Burton et al., 2015; Yuan et al., 2016; 2019a; 2020), a residual expansive clay containing  
80 about 10% in mass of interlayered illite-smectite clay (Liu et al., 2016; Yuan et al., 2016). It  
81 has a liquid limit around 70%, a plastic limit around 25% and an optimum moisture content  
82 (under standard proctor compaction) around 24% for an optimum dry unit weight of 14.7  
83 kN/m<sup>3</sup>.

## 84 3- Application of different criteria to Maryland Clay

85 Five delimiting criteria are introduced below and applied to compacted Maryland clay (See  
86 Figure 1 and Table 2):

- 87 • The “VALL” criterion (Figure 1a) consists of using the lowest point of the valley between  
88 the two peaks of a bimodal pore size distribution (PSD).
- 89 • The “CNC” criterion (Figure 1b) was proposed by Delage and Lefebvre (1984). It is based  
90 on the concept of constricted and non-constricted porosity, identified from mercury  
91 intrusion and extrusion curves.
- 92 • The “RFS” and “RCV” criteria (Figure 1c), proposed by Romero et al. (2011), stem from  
93 the observation that, upon saturation, macro pores and micro pores merge into a mono-  
94 modal distribution. The boundary between micro and macro is taken at the peak of the  
95 merged distribution. This approach applies to swelling under constant volume (RCV) and  
96 under free swell (RFS).
- 97 • The “SWRC” criterion, proposed by Romero et al. (1999), is based on the dependence of  
98 retention curves on void ratio. A delimiting diameter can be inferred by using Laplace’s  
99 equation at the value of suction corresponding to the point of convergence of retention  
100 curves.

101 The RCV, RFS and SWRC criteria are derived from the physical response of soils and rely on  
102 specific tests:

- 103 - Criteria RFS and RCV require MIP data on specimens having swollen under no applied  
104 stress (free swell) and under constant volume, respectively.
- 105 - Criterion SWRC requires at least two retention curves (at constant void ratio) in order  
106 to identify the suction at which the two curves merge.

107 These three criteria yield a “fixed” value of delimiting diameter that can then be used on  
 108 other PSDs. In contrast, VALL and CNC criteria directly reflect pore geometry and can be  
 109 applied to any PSD. As such, these values are considered as “moving” delimiting diameters.  
 110

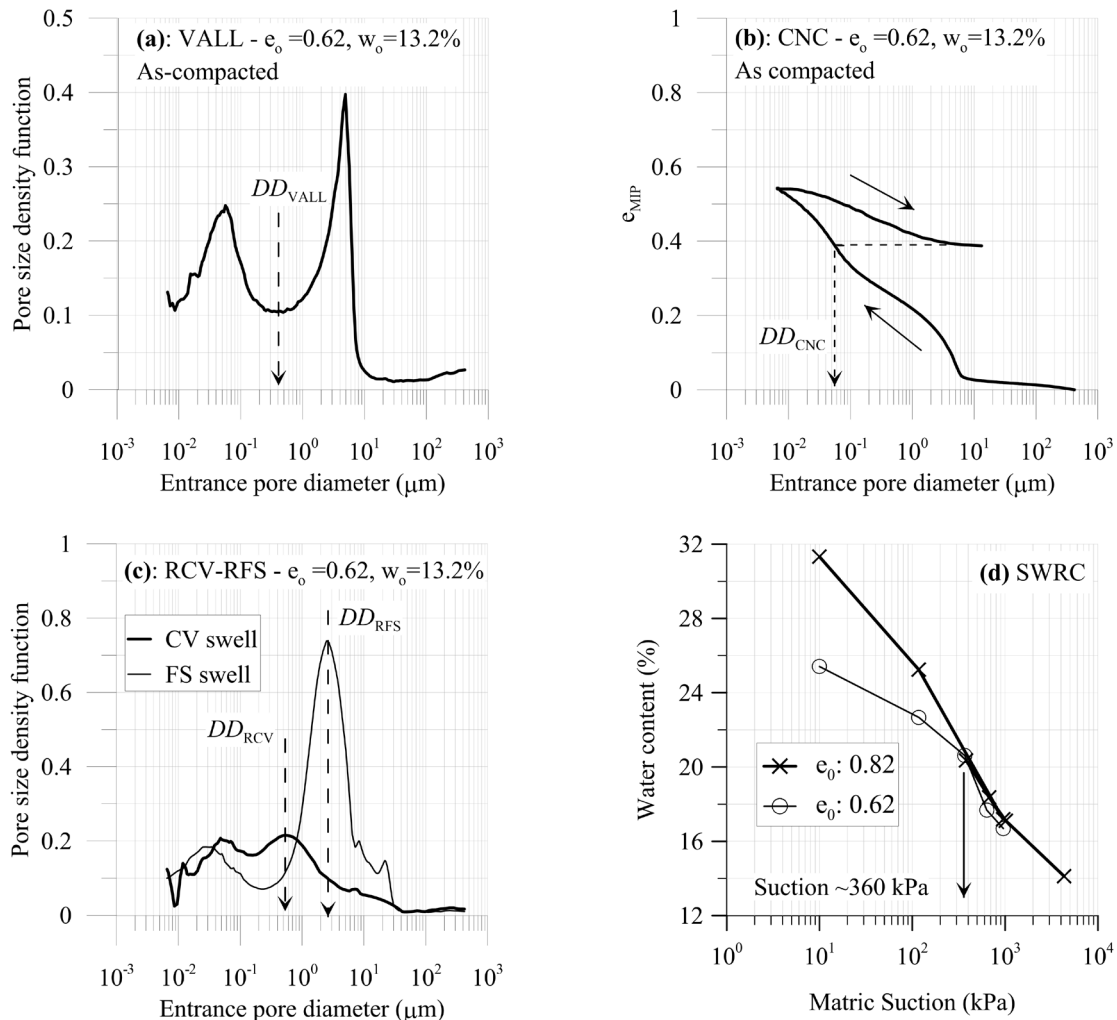


Figure 1: Criteria used to distinguish micropores and macropores, applied to pore size distribution (a-c) and retention curves (d) of Maryland clay. The pore size distributions pertain to compacted material or specimen after swelling. Information is provided, for each figure, in the legend. (a): VALL criterion, (b): CNC criterion, (c) RCV-RFS criteria, (d): SWRC criterion. Data from Yuan et al. (2016, 2019a, 2020). In the case of the VALL criterion, the midpoint is considered as the delimiting diameter ( $DD$ ) if there is a whole zone of similar low values.

111

112 The five criteria were applied to Maryland clay compacted at different values of void ratios  
 113 and gravimetric water content. For the sake of conciseness, the values of delimiting diameter  
 114 are presented only for one initial condition in Table 2. It can be seen that, depending on the  
 115 criterion selected, the delimiting diameter ranges from 0.06 to 2.5  $\mu\text{m}$ , with associated micro

116 void ratios ( $e_m$ ) ranging from 0.22 to 0.46. Consistent with Monroy et al. (2010), the CNC  
 117 criterion yields a value of 0.06  $\mu\text{m}$ , which is much lower than all other criteria and which  
 118 almost coincides with the left peak of micropores in Figure 1a. As such, we here consider that  
 119 it is not an adequate boundary and will not be discussed further in the rest of the paper.

120

121 Table 2: Summary of delimiting diameters for compacted Maryland clay (initial conditions of  
 122  $e_o = 0.62$ ,  $w_o = 13.2\%$ ) and values of micro void ratio  $e_m$ , estimated from the PSD of the  
 123 compacted soil using the delimiting diameters of each criterion.

Criterion to define delimiting diameter	VALL	CNC	RCV	RFS	SWRC*
Delimiting diameter ( $\mu\text{m}$ ).	0.40	0.06	0.60	2.5	0.8
Micro void ratio $e_m$	0.36	0.22	0.38	0.46	0.39

124 \*: calculated using Laplace's equation with a suction of 360 kPa, a water surface tension of  
 125 72.5 mN/m (at 20 degrees ) and a contact angle of 0 degree.

126

#### 127 4- Significance of boundary conditions and initial conditions for “fixed value” criteria.

128 The SWRC criterion relies on experimental retention curves determined at constant void ratio  
 129 and, as such, boundary conditions and initial water content do not really apply. However, using  
 130 a wetting branch or a drying branch to identify the merging point may affect the value of  
 131 micro/macro boundary returned by the SWRC criterion. This effect was not verified with  
 132 Maryland clay because the research conducted by Yuan et al. (2016, 2019a, 2019b, 2020)  
 133 focused on wetting paths and swelling.

134 Yuan et al. (2019a) tracked the evolution of microstructural changes in compacted Maryland  
 135 clay during wetting. Figure 2 shows the progressive merging of the two pore populations, for  
 136 free swelling and hydration under constant volume. It can be seen, in Figure 2a and 2b, that  
 137 merging is not complete and that some of the original micropores (pore size from  $10^{-2} \mu\text{m}$  to  
 138  $10^{-1} \mu\text{m}$ ) are still present in both distributions, even after full hydration.

139 Consequently, without progressive tracking of microstructural changes, the final PSD could be  
 140 interpreted as having two pore populations. i.e. micropores with pore size between  $10^{-2} \mu\text{m}$  to  
 141  $10^{-1} \mu\text{m}$  and macro pores with pore size between  $2 \cdot 10^{-1} \mu\text{m}$  to  $10 \mu\text{m}$ .

142 Using the RFS criterion on the PSD of the fully hydrated specimen (Figure 2a) returns a micro  
143 void ratio around 0.38. In contrast, considering a limit between 0.1 and 0.2 micrometer (VALL  
144 criterion), assuming that the micropores only correspond to the left peak, returns an  $e_m$  value  
145 in the order of 0.1, i.e. four times less.

146 For Boom clay, Romero et al. (2011) concluded that the boundary conditions did not affect the  
147 position of the dominant peak post-swelling. However, this is clearly not the case for Maryland  
148 clay (see Figure 2) and the difference in peak position is quite significant:  $2.5\mu\text{m}$  for free swell  
149 against  $0.6\mu\text{m}$  for constant volume.

150 Figure 3 provides further evidence that, for Maryland clay, the position of the merged peak  
151 depends on boundary conditions (Figures 3a and 3b) and initial conditions (Figure 3c) applied  
152 during swelling.

153 As expected, increasing the vertical stress on a specimen shifts the merged mono-modal peak  
154 post swelling towards smaller pore size. The effect is more pronounced for the combination of  
155 initial void ratio and initial water content that would result in most swelling, i.e.  $e_o=0.62$  and  
156  $w_o=13.2\%$  (swelling pressure in excess of 400 kPa, Yuan et al. 2016). This is because the soil  
157 compacted at  $e_o=0.82$  and  $w_o=17.8\%$  develops less swelling pressure (around 100 kPa, Yuan  
158 et al., 2016) under constant volume condition, resulting in less aggregate re-arrangement.

159 Table 3 summarizes the values of delimiting diameters obtained from the RCV, RFS and  
160 SWRC criteria for four different initial conditions for Maryland clay.

161

162

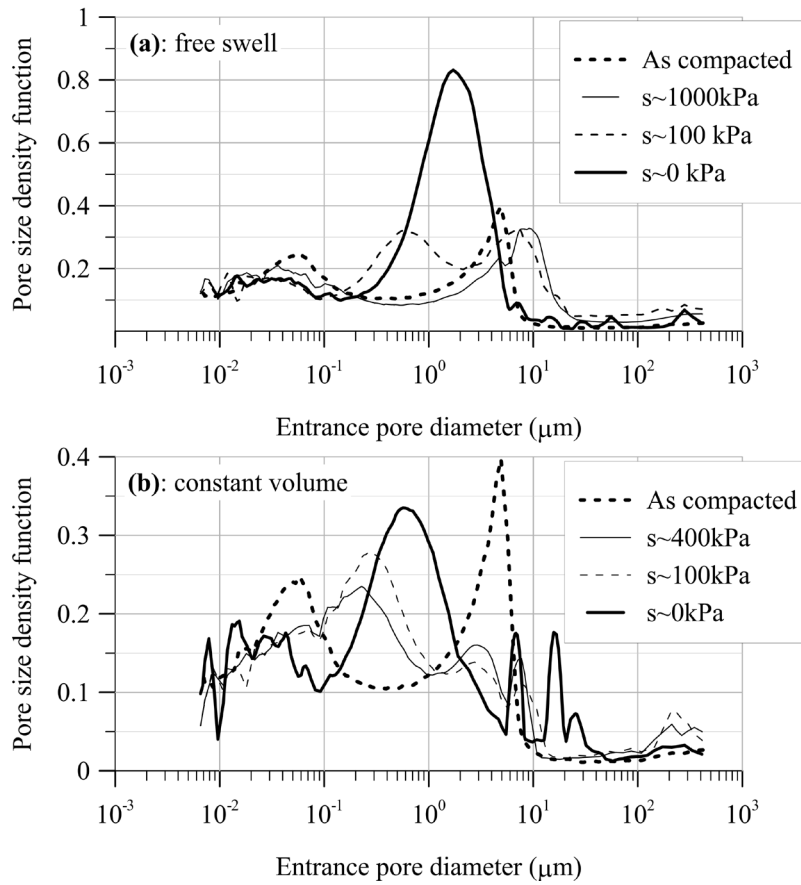


Figure 2: evolution of pore size distribution during free swelling (a) and swelling under constant volume (b). The specimen was initially compacted at  $e_o=0.62$  and  $w_o=13.2\%$ . Suction was incrementally reduced using the osmotic method. Data from Yuan et al. (2019).

163

164



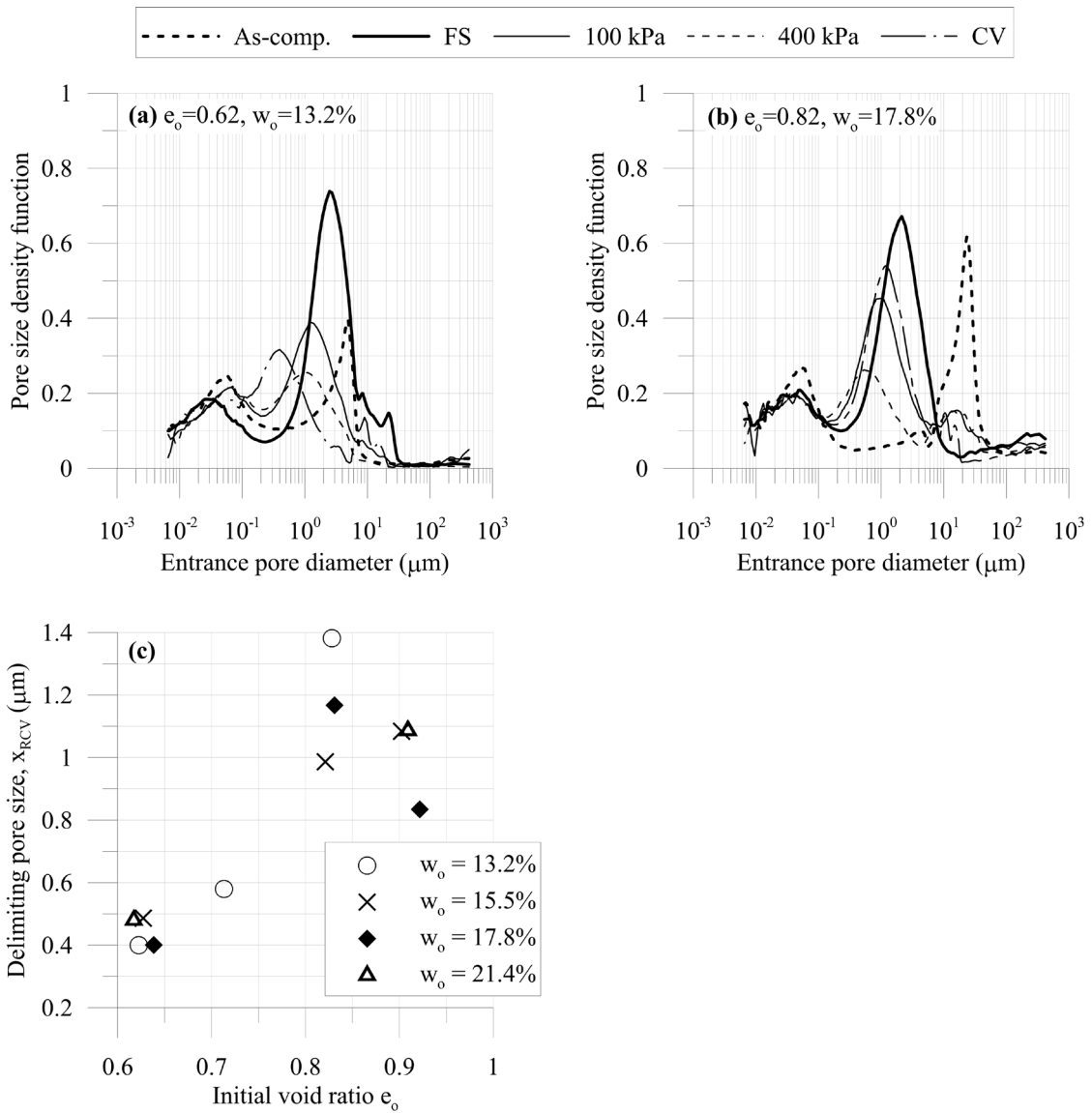


Figure 3 (a) Pore size distribution of compacted Maryland clay samples ( $e_o=0.62$ ,  $w_o=13.2\%$ ) upon swelling under different boundary conditions. FS: free swelling, CVS: constant vertical stress, CV: constant volume (after Yuan et al., 2016). (b): Pore size distribution of Maryland clay specimen ( $e_o = 0.82$ ,  $w_o = 17.8\%$ ) after compaction and following swelling under constant volume or under constant vertical stress (after Yuan et al., 2016). (c): Evolution of delimiting pore size determined by the RCV criterion with initial void ratio for compacted Maryland clay samples subjected to constant volume swelling (after Yuan et al., 2016).

168 Table 3: Summary of delimiting diameter for four different initial conditions applied to  
 169 compacted Maryland clay.

Delimiting diameter for compacted Maryland Clay ( $\mu\text{m}$ ).	$w_o = 13.2\%$		$w_o = 17.8\%$	
	$e_o = 0.62$	$e_o = 0.82$	$e_o = 0.62$	$e_o = 0.82$
RCV Criterion	0.60	0.60	0.8	1.2
RFS Criterion	2 - 2.5	1.4	1.4	2.1
SWRC Criterion	0.8			

170

171 **4- Discussion**

172 The idea behind a fixed criteria is laudable as it provides a value “once for all”, that can then  
 173 be applied to other PSDs (Romero et al., 2011). However, this idea is somewhat defeated by  
 174 the influence of initial conditions and boundary conditions. The SWRC criterion provides a  
 175 single delimiting diameter but accurately measuring retention curves at constant void ratio can  
 176 be time consuming. Another issue arises with fixed criteria if the dominant peaks shift  
 177 significantly upon swelling (see Figures 2 and 3) and drying (see Figure 4).

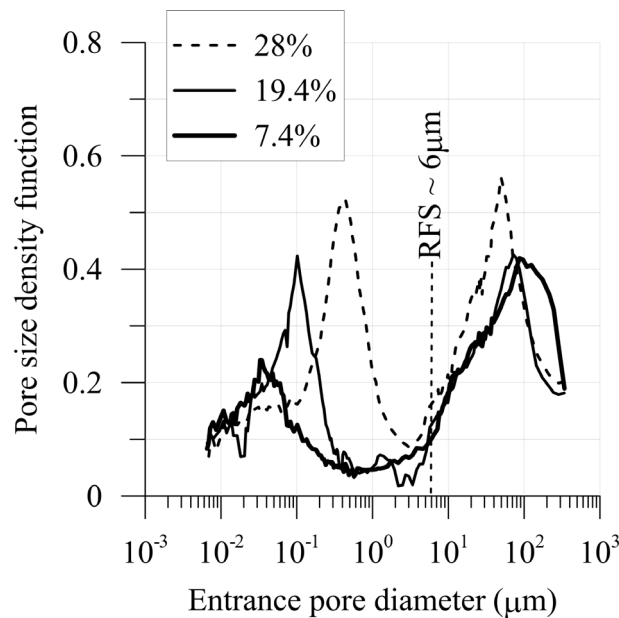


Figure 4: evolution of pore size distribution of compacted Maryland clay undergoing air-drying from initial conditions of  $w_o=28\%$ ,  $e_o=1.27$  (after Burton et al., 2015). The RFS value of 6 micrometer was estimated from swell test C10 in Burton et al. (2015).

178

179 In Figure 4, the RFS delimiting diameter clearly encroaches on the macropores, which will  
180 result in an overestimation of the micro void ratio  $e_m$ . In contrast, using a moving boundary  
181 (e.g. VALL criterion) seems more adequate to track microstructural changes.

182 It may be useful for researchers to estimate how much the micro/macro boundary may shift  
183 upon wetting and drying in order to interpret microstructural data more easily and more  
184 adequately. It was found, for Maryland clay, that the extent of pore size changes upon wetting  
185 and drying can be approximated from the microstructural data of the material compacted dry  
186 and wet of its optimum. Indeed, Figure 5 shows VALL delimiting diameters of 0.4 and 3.5  
187 micrometer for 13.1% and 32% water content, respectively, to be compared to 0.4  $\mu\text{m}$  (air  
188 drying to  $w=7.5\%$ , Figure 4) and 2.5  $\mu\text{m}$  (RCV criterion, Figure 3). Note that the position of  
189 the lowest point in Figure 5 does not depend on the void ratio achieved by compaction and is  
190 only marginally affected by the water content at high and low values of water content (see  
191 Yuan et al., 2020).

192

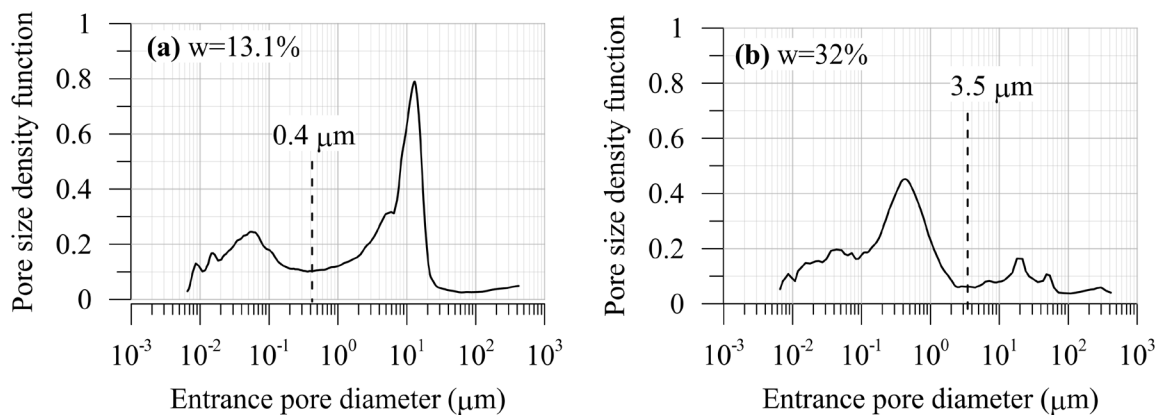


Figure 5: Pore size distribution of Maryland clay compacted to a void ratio of 0.9 with a water content of 13.1% (a) and 32% (b). The value associated with the lowest point of the valley between the pore populations is reported on each distribution. Data from Yuan et al. (2020).

193

194 For clear bimodal distributions, the adequacy of a criterion to separate micropores and  
195 macropores can easily be assessed. The criterion is used for consistency in defining the  
196 delimiting diameter. For distributions that are not clearly bimodal, it is advised to track  
197 microstructural changes with loading via successive PSDs (as per Figure 2) to help in defining

198 an adequate delimiting diameter. Special attention should be paid to cases where pore  
199 populations tend to merge, either partially or completely.

200 If pore populations can not be identified, one can question the appropriateness of trying to  
201 define micropores and macropores, especially if the results are to be interpreted in terms of  
202 inter-aggregates and intra-aggregates porosity.

203 Finally, it is suggested to account for the physical response of compacted soils when deciding  
204 on a delimiting diameter. For example, Yuan and co-workers used a value of  $1\mu\text{m}$  for Maryland  
205 clay, which allows capturing:

- 206 - The decrease of macro pores upon compaction (Delage and Graham, 1995; Lloret and Villar,  
207 2007) (Figure 6a)
- 208 - The collapse of macro pores upon wetting (Figure 6b).
- 209 - Aggregate swelling under hydration for different values of vertical stress (Figure 6c). Yuan  
210 et al. (2016) quantified the void ratio associated to the micro pores before swelling ( $e_{mo}$ ) and  
211 after a swelling phase under a constant normal stress ( $e_m$ ). A negative change in micro void  
212 ratio ( $e_m - e_{mo}$ ) reflects shrinkage of aggregates upon hydration, which is not possible and is  
213 a reflection of an inadequate delimiting diameter.
- 214 - The merging point of retention curves, as per SWRC criterion (approximately).

215 However, a  $1\mu\text{m}$  delimiting diameter is not ideal at the end of free swelling, when pore  
216 populations merge with a peak around  $2.5\mu\text{m}$ . For the fully swollen states, regardless of  
217 boundary conditions, it is recommended to align the delimiting diameter with the merged peak  
218 (similar to RFS or RCV criteria).

219

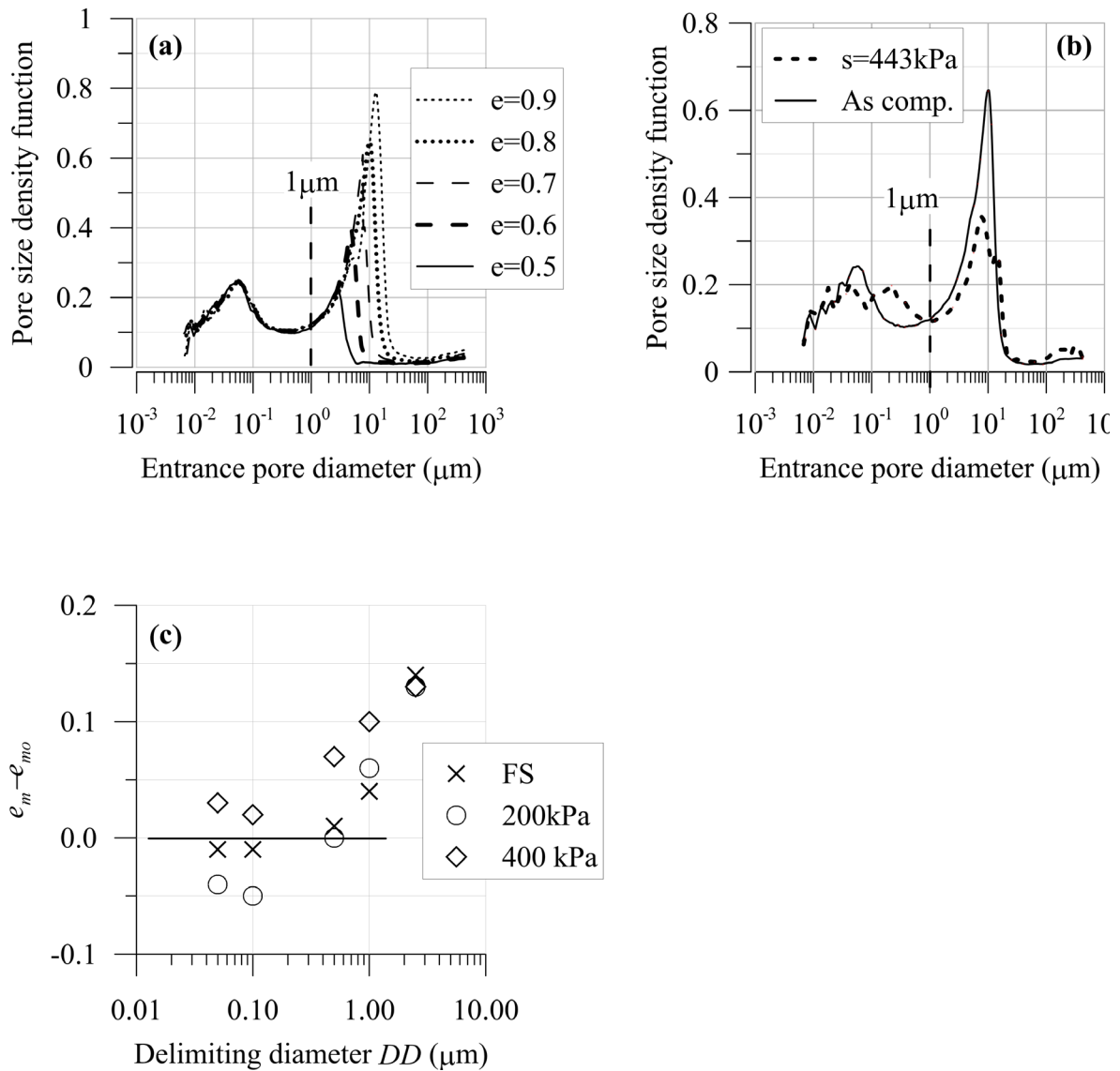


Figure 6: (a): Pore size distribution of Maryland clay compacted at a water content of 13.2% and at five different void ratios. Data from Yuan et al. (2020). (b): Pore size distribution of Maryland after compaction (initial suction of 6300 kPa, initial void ratio of 0.8) and after incremental swelling (to a suction of 473 kPa) leading to collapse. Data from Yuan et al. (2020). (c) Change in micro void ratio after free swelling and swelling under 200 kPa and 400 kPa, for different values of delimiting diameter. Data after Yuan et al. (2016).  $e_m$  is the micro void ratio at the end of swelling,  $e_{mo}$  is the micro void ratio after compaction, prior swelling.

220

#### 221 4- Conclusions

222 Several criteria have been proposed to distinguish micropores and macropores in bimodal pore  
 223 size distributions of compacted clayey soils. Five of the most commonly used criteria were

224 applied to microstructural data obtained on compacted Maryland clay undergoing swelling and  
225 drying. Three of these criteria (RFS, RCV, SWRC) return a fixed value of delimiting factor  
226 while the other two (VALL, CNC) return a moving boundary. Different criteria were found to  
227 return very different values of delimiting diameters. The criterion based on intrusion and  
228 extrusion curves significantly underestimates the micro/macro boundary. The analysis of  
229 microstructural data also showed a strong dependence of the RFS and RCV criteria to initial  
230 and boundary conditions, which defeats the idea of providing a fixed boundary. For Maryland  
231 clay, the position of dominant peaks shift significantly under wetting and drying, which fixed  
232 value criteria do not adequately capture. It is proposed to analyse successive PSDs to better  
233 track microstructural changes and define an adequate delimiting diameter. This is particularly  
234 relevant when pore populations merge upon swelling. Finally, it is advised to verify that the  
235 computed values of micro void ratio is compatible with known response of compacted clayey  
236 soils.

### 237 **Acknowledgements**

238 The authors would like to express their gratitude to the Australian Research Council (ARC) for  
239 the financial support (ARC DP110103304).

### 240 **References**

- 241 Agus S. S., Schanz T. 2005. Effect of shrinking and swelling on microstructures and fabric of  
242 a compacted bentonite-sand mixture. Proceedings of the international conference on  
243 problematic soils, Cyprus, 2, 543–550.
- 244 Ahmed S., Lovell C.W., Diamond S. 1974. Pore sizes and strength of compacted clay. J  
245 Geotech Eng Div ASCE, 100(4):407–425
- 246 Alonso E. E., Vaunat J., Gens A. 1999. Modelling the mechanical behaviour of expansive  
247 clays. Engineering Geology, 54 (1): 173–183.
- 248 Burton G.J., Pineda J.A., Sheng D., and Airey D. 2015. Microstructural changes of an  
249 undisturbed, reconstituted and compacted high plasticity clay subjected to wetting and  
250 drying. Engineering Geology, 193: 363–373.
- 251 Casini F., Vaunat J., Romero E., Desideri A. 2012. Consequences on water retention  
252 properties of double-porosity features in a compacted silt. Acta Geotechnica, 7(2): 139–  
253 150.

- 254 Casini F., Vaunat J., Romero E. 2013. A microstructural model on the link between change in  
 255 pore size distribution and wetting induced deformation in a compacted silt. In  
 256 Poromechanics V proceedings of the 5th Biot conference on Poromechanics, 1309-1313.
- 257 Delage P., Lefebvre G. 1984. Study of the structure of a sensitive Champlain clay and of its  
 258 evolution during consolidation. *Canadian Geotechnical Journal*, 21(1): 21–35.
- 259 Delage P., Graham J. 1995. The mechanical behaviour of unsaturated soils In Proceedings of  
 260 1st International Conference on Unsaturated Soils, Paris, vol 3: 1223–1256
- 261 Delage P., Pellerin F.M., 1984. Influence de la lyophilisation sur la structure d'une argile  
 262 sensible du Quebec. *Clay Minerals*. 19(2): 151–160.
- 263 Delage P., Audiguier M., Cui Y., Howatt M.D. 1996. Microstructure of a compacted silt.  
 264 *Canadian Geotechnical Journal*, 33(1):150–158
- 265 Delage P., Marcial D., Cui Y., and Ruiz X. 2006. Ageing effects in a compacted bentonite: a  
 266 microstructure approach. *Géotechnique*, 56(5): 291–304.
- 267 Della Vecchia G., Jommi C., Romero E. 2013. A fully coupled elastic-plastic  
 268 hydromechanical model for compacted soils accounting for clay activity. *International*  
 269 *Journal for Numerical and Analytical Methods in Geomechanics*, 37(5): 503–535.
- 270 Diamond, S. 1970. Pore Size Distributions in Clays. *Clays and Clay Minerals*, 18(1): 7–23.
- 271 Koliji A., Laloui L., Cuisinier O., Vulliet L. 2006. Suction induced effects on the fabric of a  
 272 structured soil. *Transport in Porous Media*, 64(2):261–278
- 273 Li X., Zhang, L. M. (2009). Characterization of dual structure pore size distribution of soil.  
 274 *Canadian Geotechnical Journal*, 46(2):129–141.
- 275 Liu X., Buzzi O., Yuan S., Mendes J., Fityus S. 2016. Multi-scale characterization of the  
 276 retention and shrinkage behaviour of four Australian clayey soils. *Canadian*  
 277 *Geotechnical Journal*, 53(5): 854-870.
- 278 Lloret A., Villar M.V. 2007. Advances on the knowledge of the thermo-hydro-mechanical  
 279 behaviour of heavily compacted “FEBEX” bentonite. *Physics and Chemistry of the*  
 280 *Earth, Parts A/B/C*, 32(8-14): 701–715.
- 281 Masin D. 2016. Development of a coupled thermo-hydro-mechanical double structure model  
 282 for expansive soils, 3rd European Conference on Unsaturated Soils, E-UNSAT 2016,  
 283 Article number 17002.
- 284 Monroy R., Zdravkovic L., Ridley A. 2010. Evolution of microstructure in compacted  
 285 London Clay during wetting and loading. *Géotechnique*, 60(2): 105–119.
- 286 Romero E., Gens A., Lloret A. 1999. Water permeability, water retention and microstructure  
 287 of unsaturated Boom clay. *Engineering Geology*, 54(1-2):117–127

- 288 Romero E., Simms P.H. 2009. Microstructure investigation in unsaturated soils: A review  
289 with special attention to contribution of mercury intrusion porosimetry and  
290 environmental scanning electron microscopy. In *Laboratory and Field Testing of*  
291 *Unsaturated Soils*. Springer Netherlands, 93–115.
- 292 Romero E., Della Vecchia G., Jommi C. 2011. An insight into the water retention properties  
293 of compacted clayey soils. *Géotechnique*, 61(4): 313–328.
- 294 Romero E. 2013. A microstructural insight into compacted clayey soils and their hydraulic  
295 properties. *Engineering Geology*, 165: 3–19.
- 296 Sánchez M., Gens A., Guimarães L., Olivella S. 2005. A double structure generalized  
297 plasticity model for expansive materials. *International Journal for Numerical and*  
298 *Analytical Methods in Geomechanics*, 29(8): 751–787.
- 299 Simms P.H., Yanful E.K. 2001. Measurement and estimation of pore shrinkage and pore  
300 distribution in a clayey till during soil-water characteristic curve tests. *Canadian*  
301 *Geotechnical Journal*, 38(4): 741–754.
- 302 Simms P.H., Yanful E.K. 2002. Predicting soil—water characteristic curves of compacted  
303 plastic soils from measured pore-size distributions. *Géotechnique*, 52(4): 269–278.
- 304 Simms P.H., Yanful E.K. 2005. A pore-network model for hydromechanical coupling in  
305 unsaturated compacted clayey soils. *Canadian Geotechnical Journal*, 42(2):499–514
- 306 Sridharan A., Altschaeffl A.G., Diamond S. 1971. Pore size distribution studies. *Journal of*  
307 *Soil Mechanics and Foundations Division*, 97(5): 771–787.
- 308 Thom, R., Sivakumar, R., Sivakumar, V., Murray, E.J., and Mackinnon, P. 2007. Pore size  
309 distribution of unsaturated compacted kaolin: the initial states and final states following  
310 saturation. *Géotechnique*, 57(5): 469–474.
- 311 Yong R.N. 1999. Overview of modeling of clay microstructure and interactions for prediction  
312 of waste isolation barrier performance. *Engineering Geology*, 54(1-2): 83–91.
- 313 Yuan S., Liu X., Buzzi O. 2018. Technical aspects of mercury intrusion porosimetry for  
314 clays. *Environmental Geotechnics*, <https://doi.org/10.1680/jenge.16.00039>.
- 315 Yuan S., Liu X., Buzzi O. 2019b. Effects of soil structure on the permeability of saturated  
316 Maryland clay. *Géotechnique*, 69(1), 72-78.
- 317 Yuan S., Liu X., Buzzi O. 2020. A microstructural perspective into soil collapse.  
318 *Geotechnique*, <https://doi.org/10.1680/jgeot.18.P.256>.
- 319 Yuan S., Buzzi O., Liu X., Vaunat J. 2019a. Swelling behaviour of Maryland clay under  
320 different boundary conditions. *Géotechnique*, 69(6), 514-525.
- 321 Yuan S., Liu X., Sloan S.W., Buzzi O.P. 2016. Multi-scale characterization of swelling  
322 behaviour of compacted Maryland clay. *Acta Geotechnica*, 11(4): 789-804.



323 Zimmie, T.F., Almaleh, L.J., 1976. Shrinkage of Soil Specimens During Preparation for  
324 Porosimetry Tests, in: Soil Specimen Preparation for Laboratory Testing, ASTM STP  
325 599. American Society for Testing and Materials, 202–215.